

MR fingerprinting based on realistic vasculature in mice: identifiability of physiological parameters

Philippe Pouliot^{1,2}, Louis Gagnon¹, Tina Lam⁴, Pramod Avti⁵, Michèle Desjardins¹, Ashok Kakkar⁴, Sava Sakadzic³, David Boas³, and Frédéric Lesage¹

¹Electrical Engineering, Ecole Polytechnique Montreal, Montreal, QC, Canada, ²Research Centre, Montreal Heart Institute, Montreal, QC, Canada, ³Athinoula A. Martinos Center for Biomedical Imaging, Massachusetts General Hospital, Harvard Medical School, MA, United States, ⁴Chemistry Department, McGill University, QC, Canada, ⁵Montreal Heart Institute, QC, Canada

TARGET AUDIENCE: Scientists interested in realistic modeling of the magnetic resonance (MR) signal.

PURPOSE: MR vascular fingerprinting is a novel approach to estimate cerebral blood volume, mean vessel radius, and oxygenation maps in the human brain¹ using one pre and one post injection scans. To our knowledge, this approach has not yet been fully validated. Here we implemented for the first time the sequence in mice (Fig. 1), and exploited a dictionary built on simulations of the MR signal based on realistic vasculature.

METHODS: A multi-slice 2D GESFIDE² sequence was implemented and tested on doped water phantoms on a 7T Agilent 30cm bore scanner (TR/TE1/TE2=3s/2ms/1.8ms, 36 echoes, 180 pulse after 12th echo, 12 slices, 128x128 matrix, 4 reps, 25 min per scan), and robust data in 6 mice were acquired, with 2

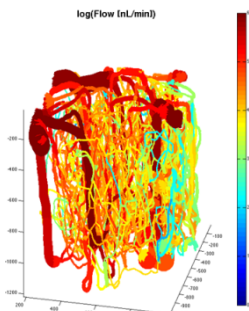


Fig. 2: Vessel size and flow in mouse 2-photon angiogram

mice under a protocol of hypercapnia (5% CO₂ in 30% O₂) and 4 mice under injection of SPIONs through the tail vein (2mM, 0.2 ml). Using proton Monte-Carlo simulations of spin evolution³, with $2 \cdot 10^6$ protons and time step of 0.2 ms, the MR signal for GESFIDE was simulated in voxels based on 2-photon angiograms (Fig. 2) acquired in 6 other mice. For each angiogram, a dictionary $M=f(P)$ for fingerprint extraction with about 100 entries was generated by sparsely sampling along 5 parameters (P): hemoglobin oxygen saturation, vessel radius, capillary density, SPION concentration and large scale magnetic field inhomogeneity. Preliminary brain maps of the above quantities were extracted by

fitting the experimental fingerprints to the dictionary. By linearizing $M=f(P)$ ($\rightarrow \Delta M/M_0 = \Delta P$ for baseline M_0), the dictionary eigensystem was characterized to study its degeneracies in realistic vascular conditions.

RESULTS: Fig. 3 shows boxplots of the eigenvalues of A with spread due to angiograms from several mice. This confirmed that all the eigenvalues are positive and distinct, and therefore all parameters studied are theoretically identifiable. However the eigenvalues span 4 orders of magnitude, leading to estimability issues in the presence of noise. Despite using different angiograms, similar eigenvalue profiles were obtained without outliers. Fig. 4 shows the distribution of A in measurement space. Curves are shown to be similar for the different angiograms, but are noticeably different for different physiological parameters.

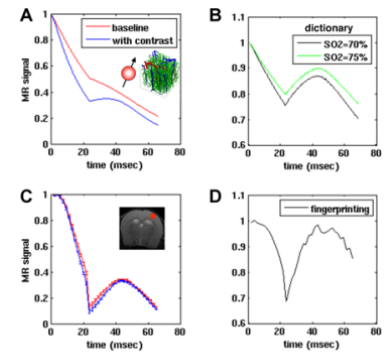


Fig. 1: MR fingerprinting in mouse brain

fitting the experimental fingerprints to the dictionary. By linearizing $M=f(P)$ ($\rightarrow \Delta M/M_0 = \Delta P$ for baseline M_0), the dictionary eigensystem was characterized to study its degeneracies in realistic vascular conditions.

DISCUSSION: As a next step, simulation results presented in this abstract will be optimized to extract accurate parameter maps from the experimental data. Each dictionary entry took about 30 minutes to generate, in a process that can be highly parallelized confirming the feasibility of this approach. In our preliminary fits using 7T MR acquisitions in mice, significant T1 effects were observed that require further investigations.

CONCLUSION: Additional acquisitions are planned and the generation of a dictionary with 100 times more entries. The main objectives of extracting robust oxygenation and other parameter maps from mice brains using MR fingerprinting remain to be tackled.

REFERENCES: ¹Christen, T. et al., NeuroImage 89 (2014) 262-270. ²Ma and Wehrli, JMR B111 (1996) 61-69. ³He and Yablonskyi, MRM 57 (2007) 115-126.

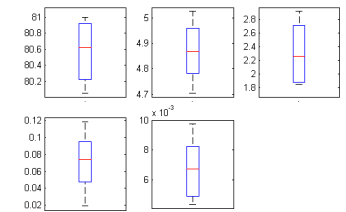


Fig. 3: Distributions of eigenvalues of A .

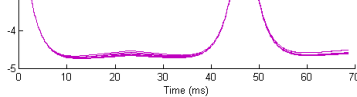


Fig. 4: Distributions of rows of A